JOURNAL OF VIROLOGY, July 2005, p. 8149–8163 Vol. 79, No. 13
0022-538X/05/$08.00+0 doi:10.1128/JVI.79.13.8149–8163.2005

Promoters, Transcripts, and Regulatory Proteins of Mungbean Yellow Mosaic Geminivirus†

P. V. Shivaprasad,[2] Rashid Akbergenov,[1] Daniela Trinks,[3] R. Rajeswaran,[2] K. Veluthambi,[2] Thomas Hohn,[1,3]* and Mikhail M. Pooggin[1]*

Institute of Botany, University of Basel, Schönbeinstrasse 6, CH-4056 Basel,[1] and Friedrich Miescher Institute for Biomedical Research, Maulbeerstrasse 66, CH-4058 Basel,[3] Switzerland, and School of Biotechnology, Madurai Kamaraj University, Madurai-625021, India[2]

Received 12 November 2004/Accepted 2 March 2005

Geminiviruses package circular single-stranded DNA and replicate in the nucleus via a double-stranded intermediate. This intermediate also serves as a template for bidirectional transcription by polymerase II. Here, we map promoters and transcripts and characterize regulatory proteins of *Mungbean yellow mosaic virus-Vigna* (MYMV), a bipartite geminivirus in the genus *Begomovirus*. The following new features, which might also apply to other begomoviruses, were revealed in MYMV. The leftward and rightward promoters on DNA-B share the transcription activator AC2-responsive region, which does not overlap the common region that is nearly identical in the two DNA components. The transcription unit for BC1 (movement protein) includes a conserved, leader-based intron. Besides negative-feedback regulation of its own leftward promoter on DNA-A, the replication protein AC1, in cooperation with AC2, synergistically transactivates the rightward promoter, which drives a dicistronic transcription unit for the coat protein AV1. AC2 and the replication enhancer AC3 are expressed from one dicistronic transcript driven by a strong promoter mapped within the upstream AC1 gene. Early and constitutive expression of AC2 is consistent with its essential dual function as an activator of viral transcription and a suppressor of silencing.

The family *Geminiviridae* comprises small circular single-stranded DNA viruses that cause severe diseases in major crop plants worldwide. On the basis of genome organization, host range, and type of insect vector, the family is divided into four genera: *Mastrevirus*, *Curtovirus*, *Topocuvirus*, and *Begomovirus* (42). Members of the largest genus, *Begomovirus* (10), infect primarily dicotyledonous plants and are transmitted by the whitefly *Bemisia tabaci*. Many begomoviruses have a bipartite genome, with a DNA-A component encoding all the protein functions necessary for virus replication in a single cell while the DNA-B component provides movement functions required for systemic spread.

Transcription regulation in begomoviruses has been extensively studied in both transgenic plants (13, 19, 23, 40, 48, 60) and protoplast systems (8, 9, 13, 16, 17, 24, 46, 47, 49, 51, 52, 53, 60). Transcription start and poly(A) sites on both DNA-A and -B have been partially or completely mapped for *African cassava mosaic virus* (ACMV) (54), *Tomato golden mosaic virus* (TGMV) (19, 36, 45, 50), *Abutilon mosaic virus* (AbMV) (14), and the monopartite *Tomato leaf curl virus* (TLCV) (34). However, major gaps in our understanding of the structural organization of begomovirus promoters and transcription units, and of the regulation of transcription by viral proteins, remain. Bidirectional promoters have been identified in the intergenic regions (IGR) of DNA-A and DNA-B, which share a common region (CR) of about 160 to 200 bp. The CR includes all *cis*-acting elements required for DNA replication and a core promoter driving leftward transcription of the AC1 gene encoding the replication-associated protein (Rep) (reviewed in reference 20). AC1 also functions as a negative-feedback regulator of transcription from its own promoter (16, 17, 24, 51) by binding to iterative sequences (iterons) located within the CR between the TATA box and the AC1 transcription start site (9, 11, 12). Much less understood is the expression mechanism of the downstream leftward genes AC2 (encoding the transcriptional activator protein [TrAP], also involved in suppression of silencing) and AC3 (encoding the replication enhancer [REn]), especially the regulatory role of CR-based transcription elements.

Begomovirus AC2 is a viral transcription factor that transactivates the late viral genes AV1 (encoding coat protein [CP]) and BV1 (encoding nuclear shuttle protein [NSP]) on DNA-A and DNA-B, respectively (17, 47). We have recently shown that *Mungbean yellow mosaic virus-Vigna* (MYMV-Vig; referred to below as MYMV) AC2 and its ACMV homolog also transactivate several plant genes (55). The molecular mechanism of transactivation remains unknown, and attempts to identify a single *cis* element conserved in all AC2-responsive promoters have met with little success (2, 40, 49). In MYMV, ACMV, and other Old World begomoviruses, the AV1 gene is overlapped at the 5′ end by an open reading frame (ORF) of unknown function (AV2), and the mechanism of transcription and translation of these overlapping genes is not understood. Likewise, a mechanism for expression (if any) of the AC4 ORF embedded within the AC1 gene is not known. Finally, in DNA-B, the bidirectional promoter elements and the transcription start site in the leftward direction have not been mapped unambiguously (14, 17, 45, 54, 60). In this work we have attempt-

* Corresponding author. Mailing address: Institute of Botany, University of Basel, Schönbeinstrasse 6, CH-4056 Basel, Switzerland. Phone: 41 61 2672977. Fax: 41 61 2673504. E-mail for Thomas Hohn: hohn@fmi.ch. E-mail for Mikhail M. Pooggin: Mikhail.Pooggin@unibas.ch.

† Supplemental material for this article may be found at http://jvi.asm.org/.

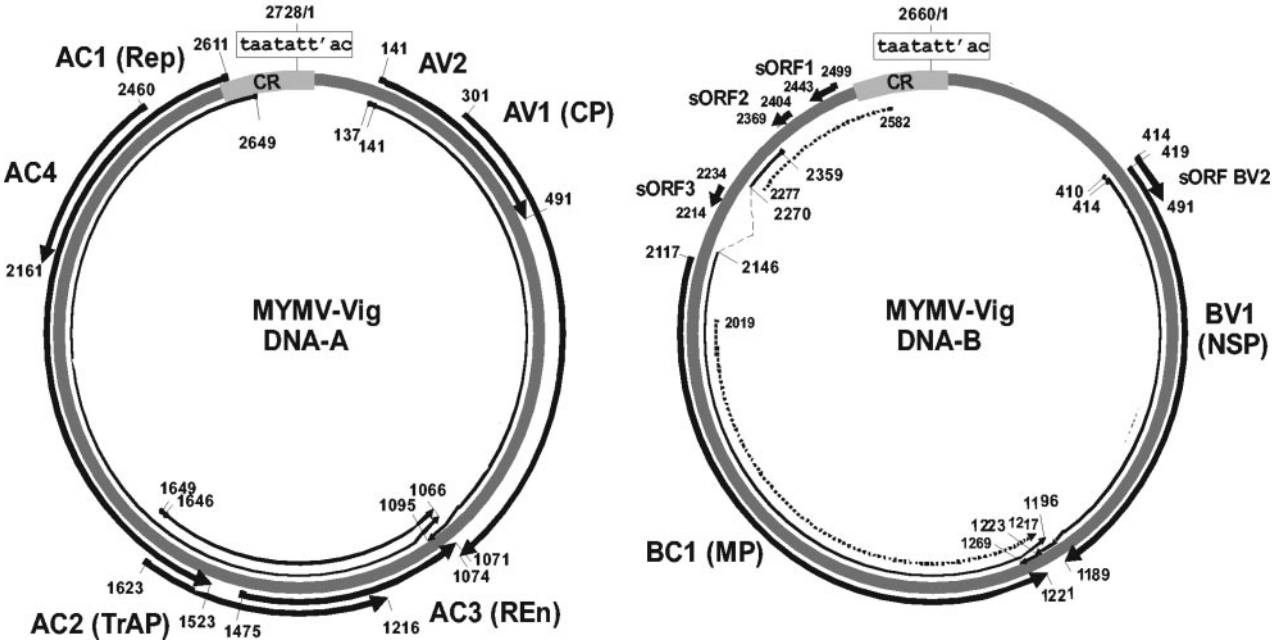

FIG. 1. Genome and transcriptome of MYMV. The MYMV bipartite genome comprises two components, DNA-A and DNA-B (variant KA22) (gray circles), of 2,728 and 2,660 nt, respectively, which share a CR containing an invariant nonanucleotide (boxed) with a nick site (indicated between t and a; the numbering starts from the latter nucleotide). Rightward- and leftward-oriented ORFs, encoded on the viral and complementary stands, respectively, are shown as thick arrows with the names of their products. The major transcription units mapped in this work are depicted as thin arrows, with positions of the major transcription start sites and poly(A) sites indicated. The minor DNA-B transcript is shown by a dotted line and the intron found in the major BC1 transcript by a dashed line.

ed to address these and other unresolved issues to draw a more complete picture of the begomovirus "transcriptome" and its regulation both in *cis* and in *trans*.

MYMV is a bipartite begomovirus isolated from infected blackgram (*Vigna mungo* L. Hepper) in Tamil Nadu, India (57). Interestingly, this virus has a highly variable DNA-B component, with MYMV DNA-A supporting replication of any one of five distinct DNA-B species (27). In agroinoculation experiments, symptom severity depended on the B-component used (3, 27). Here, we map transcripts of MYMV comprising DNA-A and one of the DNA-B variants (KA22) (Fig. 1) from agroinfected blackgram plants. Potential promoters, transcription units, and regulatory proteins of this virus were characterized in a *Nicotiana plumbaginifolia* leaf protoplast transient expression system.

MATERIALS AND METHODS

Virus and plant infection. Blackgram [*Vigna mungo* (L.) Hepper] plants were infected with MYMV by agroinoculation of germinating seeds as described previously (26). A single *Agrobacterium tumefaciens* strain Ach5 harboring two compatible replicons with the partial tandem repeats of MYMV DNA-A (AJ132575) and DNA-B (AJ132574) was used, which gives 100% infection efficiency (26). The plants were grown in a phyto-chamber (Sanyo, Osaka, Japan) with a light and dark cycle of 16 and 8 h, respectively, at 25°C.

RNA extraction and cRT-PCR. Total RNA was extracted from young (uppermost) symptomatic trifoliate leaves of infected blackgram plants about 3 to 4 weeks postinoculation, using a Trizol reagent (Gibco-BRL, Scotland) followed by further purification with an RNeasy Plant minikit (QIAGEN, Hilden, Germany) as recommended by the manufacturers. A circularization-reverse transcription–PCR (cRT-PCR) method (6) was applied to coamplify 5′ and 3′ termini of all potential viral transcripts. First, 5′-capped RNA was decapped by incubating 10 μg of total RNA with 10 U of tobacco acid pyrophosphatase (Epicentre Technologies, Madison, WI) and 20 U of the RNase inhibitor RNasin (Promega) in a total volume of 20 μl buffer (50 mM sodium acetate [pH 6.0], 1 mM EDTA, 0.01% Triton X-100, 0.1% β-mercaptoethanol) for 1 h at 37°C. RNA circularization was performed by diluting the 20-μl sample of decapped RNA to 400 μl with 1× T4 RNA ligase buffer (50 mM Tris-HCl [pH 7.5], 10 mM $MgCl_2$, 20 mM dithiothreitol [DTT], 100 μM ATP, 100 μg/ml acetylated bovine serum albumin) and incubating with 20 U of T4 RNA ligase (NEB) and 40 U of RNasin (Promega) for 16 h at 16°C. After extraction with phenol-chloroform–isoamyl alcohol (25:24:1), RNA was precipitated with ethanol. Reverse transcription was performed as follows. The RNA pellets after ligation were dissolved in 22 μl sterile bidistilled water, mixed with 2 μl of 10-pmol/μl RT primer (primer sequences given in Fig. 4 to 6), incubated at 70°C for 10 min, and chilled on ice for 5 min. The sample was split in two, and each 12-μl portion was added to a 4-μl mixture of 5× first-strand synthesis buffer (250 mM Tris-HCl [pH 8.3], 375 mM KCl, 15 mM $MgCl_2$, 0.1 M DTT), 2 μl 0.1 M DTT, and 1 μl 10 mM deoxynucleoside triphosphate mix, incubated at 42°C for 2 min, and then further incubated at 42°C for 50 min with either 1 μl of 200-U/μl SuperScriptII RNase H^- reverse transcriptase (Gibco BRL) or 1 μl of sterile water (as a control). PCR amplification with a pair of 5′ and 3′ primers specific for each transcription unit (indicated in Fig. 4 to 6) was performed in 100 μl 1× PCR buffer with 2 U of *Taq* DNA polymerase (NEB) and 1/20 of the reverse transcription reaction mixture as a template for 40 cycles (each cycle consisting of 30 s at 95°C, 30 s at 52°C, and 45 s at 72°C). Amplification products were analyzed by 1.5% agarose gel electrophoresis. The region corresponding to amplified cDNA, which usually appeared as a diffuse band or a smear due to the varying length of poly(A) stretches, was excised from the gel and cloned.

Cloning and sequencing of cRT-PCR products. PCR products were purified using a gel extraction kit (QIAGEN), trimmed with XhoI and SphI (or EcoRI, in the case of the BC1 transcription unit, which contains a unique SphI site at position 2401; besides the latter, there are no other SphI or XhoI sites in DNA-A or -B of MYMV), and cloned into XhoI and SphI (or EcoRI) sites of pKS_{XAHA} (38). Sequencing of individual clones with primer #1 (5′-GTG GAT TGA TGT GAT ATC TCC ACT G-3′), which reads from upstream of the XhoI site of the vector, was performed using an automatic sequencer (ABI model 377). The sequence runs representing all the transcription units mapped here are shown in Fig. S1 and S2 in the supplemental material.

Plasmid constructs. Promoter segments of the MYMV genome (DNA-A, AJ132575; DNA-B, AJ132574) were subcloned by PCR into the Amp^r plasmid

pKS_{XAHA} (38) in place of the region comprising the Cauliflower mosaic virus (CaMV) 35S promoter and S1 leader, between AflIII and NcoI sites. In the resulting constructs, the MYMV promoter region up to the first ATG codon of the viral ORF is fused directly (i.e., through the NcoI site containing the ATG) to a chloramphenicol acetyltransferase (CAT) reporter coding sequence, followed by the CaMV terminator. In all the promoter constructs, the initiation context of the ATG start codon is optimal (29), i.e., with a purine at position −3 and a guanosine at position +4, with respect to the first nucleotide of the ATG [(**A**/**G**) (C/A) C **ATG G**] (see Table S1 in the supplemental material).

At the 5′ borders of most bidirectional promoter segments, the vector AflIII site (not restored due to the blunt-end ligation) is adjacent to an EcoRI site followed by the viral sequence (ACATGAATTCn. . . [EcoRI site underlined; n, viral nucleotide]) from the following genome positions (corresponding to "n"): A-2613, for constructs AC1–AV2 and AC1–AV1; A-2464, for AC4–AV2 and AC4–AV1; A-128, for AV2–AC1 and AV2–AC4; A-300, for AV1–AC1 and AV1–AC4; B-2119, for BC1–BV1 and BC1[-CR]BV1; and B-417, for BV1–BC1 and BV1[-CR]BC1. A precise deletion of the most conserved 134-bp sequence of the CR from the CAT constructs BC1–BV1 and BV1–BC1 was performed by PCR ligation, creating a new unique AflIII site at the junction (t2551-ACATGt26 [the new site is underlined]), thus yielding BC1[-CR]BV1 and BV1[-CR]BC1. The AflIII-NcoI fragments of the latter two constructs were subcloned into the original vector pKS_{XAHA}, yielding BV1short and BC1short, respectively. AC2::CAT and AC3::CAT fusion constructs were created by cloning the corresponding regions (amplified with PCR and trimmed with AflIII [the sites imbedded in both PCR primers]) into the AflIII and NcoI sites of pKS_{XAHA} (for the resulting ATG contexts, see Table S1 in the supplemental material). The 5′ borders of the resulting AC2 promoter versions, adjacent to the restored AflIII site (ATATGT) of the vector, correspond to the following genome positions: A-298, for constructs AV1–AC2 and AV1–AC3; A-2607, for AC2[-IGR] and AC3[-IGR]; and A-1978, for AC2short and AC3short. A point mutation of the AC2 start codon (ATG to TAG) was introduced into construct AC3short by PCR ligation, yielding AC3short[–AC2atg].

The coding regions of the AC1, AC2, and AV1 genes (DNA-A positions 2611 to 1523, 1623 to 1216, and 301 to 1074, respectively) and the BC1 and BV1 genes (DNA-B positions 2117 to 1221 and 419 to 1189, respectively) were introduced by PCR between the XhoI and SphI sites of pKS_{XAHA} in place of the CAT reporter, yielding p35SAC1, p35SAC2, p35SAV1, p35SBC1, and p35SBV1, respectively. The following pairs of primers were used: for AC1, 5′AAAACCTCGAGaaaatatgcctagactcggtcg (XhoI and start codon underlined; viral nucleotides in lower case) and 5′ACCCAGCATGCaaatcaattcgagagcgtcgaattgctc (SphI and stop codon underlined); for AC2, 5′TTGTGCTCGAGaaagaatgcggaattctacaccctc and 5′ATTTAGCATGCtcactaaaagtcgataatatcatcccag; for AV1, 5′TTACGCTCGAGgaaacatgccaaagcggaattacg and 5′CAATAGCATGCttattaatttgaaatcgaatc; for BC1, 5′ACACACTCGAGgaataatggagaattattcagg and 5′ATAAAGCATGCgtgttacaacgctttgttcac; and for BV1, 5′GTTTTCTCGAGtgAaaatgtttaaccgcaatta tcgc and 5′TATTCGCATGCatttttatcccacgtatttcaattc.

Note that the MYMV sequence used in this study was found to differ at two sites from the GenBank-deposited DNA-A (AJ132575; the stretch 1981-gcgcga gct-1990 is replaced by 1981-gCcgcgagcGGt-1993—an insertion of 3 nucleotides [nt]) and DNA-B (AJ132574; 2191-tacgcgagcg-2200 is replaced by 2191-taGgcC GCGCagcg-2204—an insertion of 4 nt and substitutions at two positions) sequences. These two differences were confirmed by sequencing of the original infectious clone and, for DNA-B, also of cDNA from infected plants. All genomic positions in this paper refer to the corrected complete sequences of DNA-A and DNA-B.

Transient expression in plant protoplasts. Protoplasts from leaf tissue of *Nicotiana plumbaginifolia* plants were prepared as described previously (15). A 300-μl aliquot of protoplasts (6×10^5) was transfected with up to 30 μl plasmid DNA (in sterile bidistilled water containing 10 μg CAT plasmid, 10 μg viral protein expression plasmid [e.g., AC2, AC1, or AC1 plus AC2], and 2 μg 35S–β-glucuronidase [GUS] plasmid as an internal control of transfection efficiency) by polyethylene glycol-mediated transfection as described previously (15, 55). Following incubation for 19 to 24 h at 28°C in the dark, protoplasts were harvested, and protein extracts were prepared and assayed for CAT and GUS activity as described previously (55). Relative GUS activities were taken for normalization of CAT expression levels. For each construct, the values given are the means of at least four independent batches of protoplasts. Deviations from the mean values did not exceed 30%. The statistical significances of changes in expression in response to the regulatory proteins were validated by Student's *t* test (data not shown).

Northern blot hybridization. For Northern blot analysis, two parts of the MYMV-infected blackgram seedlings, which contained the first unopened and not fully opened leaf buds, up to 1.5 cm (sample 2), and the first fully opened trifoliate leaves, about 3 cm (sample 3), as well as a control sample of the uppermost, healthy blackgram leaves (sample 1), were taken. Total RNA was isolated from 0.5 g tissue by the Trizol method, as described above for cRT-PCR. One hundred micrograms of total RNA was treated with RNase-free DNase I (Amersham), as recommended by the manufacturer, then purified twice with phenol-chloroform (1:1), precipitated with ethanol, and dissolved in 70 μl diethyl pyrocarbonate-treated water. RNA blot hybridization was performed as described previously (35). Briefly, 10 μg total RNA was separated in a 1.5% agarose gel with 1.1% formaldehyde, transferred to a nylon membrane (Hybond N+; Roche), and UV cross-linked. As probes, the viral DNA fragments (DNA-A positions 1446 to 2725, AC1 probe; 1194 to 1671, AC2; 147 to 1103, AV1; and DNA-B positions 415 to 1192, BV1; 1218 to 2122, BC1) containing the respective full-length viral genes were labeled with [α-^{32}P]dCTP (Board of Radiation and Isotope Technology, Government of India) by random primers using a Megaprime TM labeling kit (Amersham). Hybridization was performed at 42°C for 20 h. Following stringent washing, the membranes were exposed to Kodak films at −70°C for 16 h (for the AC1 probe) or 8 h (for the AC2, AV1, BV1, and BC1 probes).

RESULTS

The bidirectional promoters of MYMV and their regulation. To investigate regulation of the bidirectional transcription controlled by the IGR of MYMV DNA-A and DNA-B, CAT reporter fusions were constructed with both orientations of several IGR versions spanning the sequences between the first AUG start codons of the individual leftward- and rightward-oriented ORFs (Fig. 2). Expression from these constructs was assayed in a transient expression system based on protoplasts from *N. plumbaginifolia* leaves. A plasmid constitutively expressing the GUS reporter gene was routinely cotransfected to serve as an internal standard to monitor transfection efficiency and to normalize CAT expression levels. Note that, in our experimental system, plasmid DNA carrying a viral promoter region, when delivered into the plant protoplast nucleus, mimics the viral circular double-stranded DNA that serves as a template for bidirectional transcription in naturally infected plant cell nuclei. With the exception of negligible expression from the BV1 start codon, all the constructs drove low levels of CAT expression (Fig. 2, open bars), ranging from 0.2 to 1.5% of that driven by the strong constitutive CaMV 35S promoter, with basal leftward expression from the AC1 start codon being the highest (1.4 to 1.5% [Fig. 2]).

In other begomoviruses, the AC2 protein acts as a transcription activator of late viral genes, i.e., rightward genes from DNA-A and all genes from DNA-B (13, 17, 47). Consistently, coexpression of MYMV AC2 from a separate plasmid dramatically activated expression of CAT fused to the start codons of the AV2, AV1, BC1, and BV1 genes (15- to 300-fold) (Fig. 2, black bars), thus achieving up to 33.1% (BV1) of the level of the 35S promoter, which itself was not significantly affected by AC2. Somewhat less expectedly, leftward expression from DNA-A was also increased, albeit less dramatically (two- to fourfold).

Similar patterns of basal expression and AC2-mediated transactivation were also observed when the MYMV DNA-A and DNA-B promoters were fused to a firefly luciferase reporter and tested in both *N. plumbaginifolia* and *Orychophragmus violaceus* protoplasts (data not shown).

Even in the presence of AC2, CAT expression from the AC4 start codon was very low. These low levels might be explained by inefficient leaky scanning translation from the AC1 mRNA (see below). However, we cannot exclude that a sequence downstream of the AC4 start codon (not included in our con-

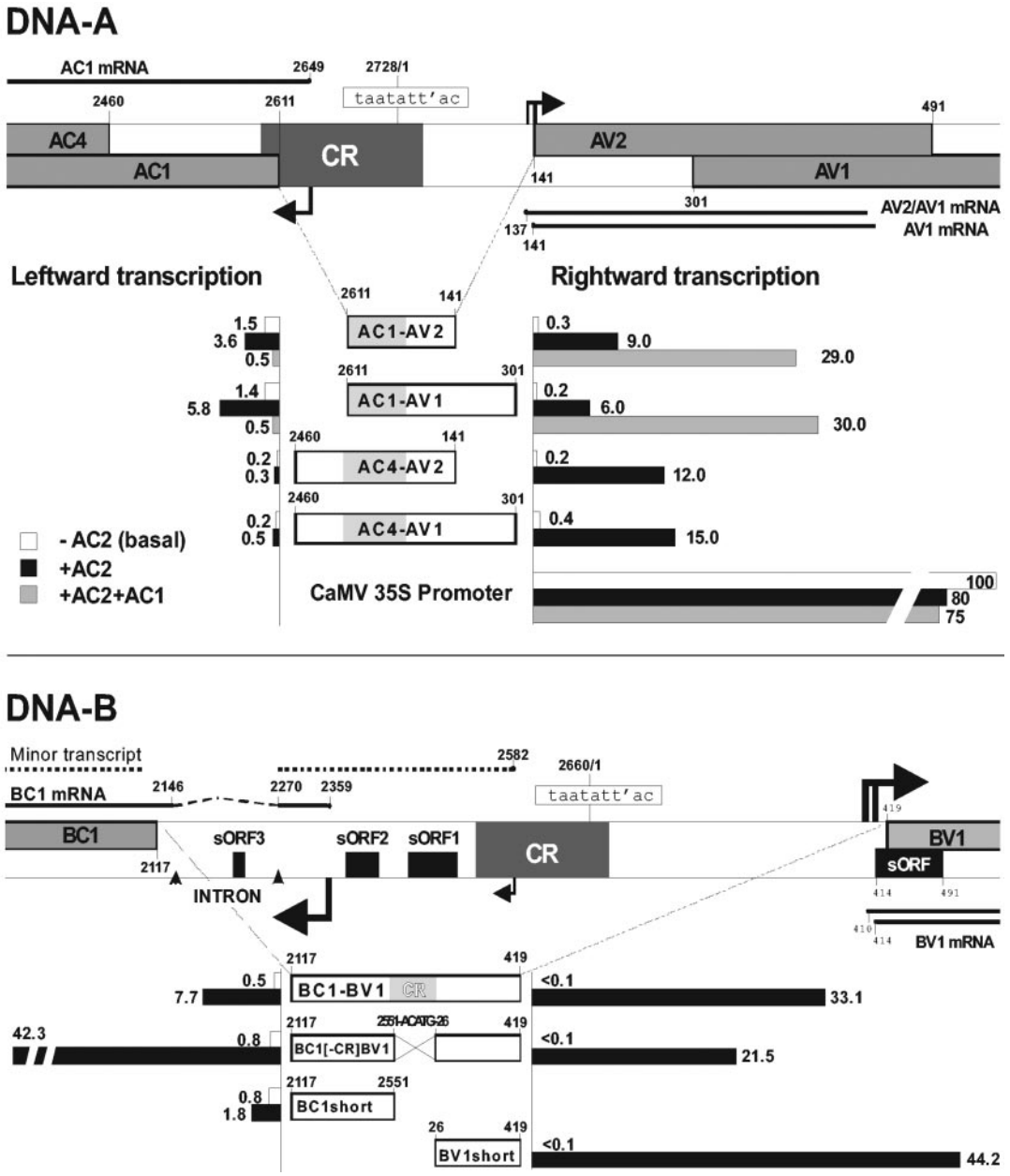

FIG. 2. Mapping of the bidirectional promoters in the intergenic regions of MYMV DNA-A and DNA-B. Schematic representations of DNA-A (top) and DNA-B (bottom) IGR-containing sequences. Rightward- and leftward-oriented ORFs (gray outlined boxes, or black boxes for sORFs), the CR with the invariant nonanucleotide (boxed), the major transcription start sites (bent arrows), and the corresponding transcripts (thick lines) are depicted and their genomic positions indicated. For DNA-B, the minor transcript (see also Fig. S2, panel C, in the supplemental material) is indicated by a dotted line, with the start site shown by a small bent arrow. The intron in the major transcript is indicated, with arrowheads indicating the positions of the splice sites. The promoter segments fused to a CAT reporter in both orientations and tested in *N. plumbaginifolia* protoplasts are shown below each scheme (names of constructs and flanking nucleotide positions as indicated), and the CAT expression levels (mean values) obtained in the absence of regulatory proteins and in the presence of AC2 or (in the case of AC1–AV2 and AC1–AV1) AC2 plus AC1 proteins are given relative to a 35S-CAT control. Note that background expression in mock-transfected protoplasts, subtracted prior to calculation of the relative CAT levels, did not exceed 0.2% of the 35S-CAT control.

structs) may contribute to AC4 expression in the normal viral context.

In DNA-A, the core promoter driving leftward transcription is located within the region common to both MYMV DNAs (CR). To test the contribution of the CR to the bidirectional promoter activity in DNA-B, a 134-bp noncoding portion of the 167-bp DNA-B CR, which has only one mismatch to the corresponding sequence of DNA-A and contains a consensus TATA box, was deleted from the 962-bp DNA-B IGR segment tested above. Only a slight reduction of rightward expression from the BV1 start codon in the presence of AC2 was observed, and its basal level remained below reliable detection (<0.1% of the 35S promoter [Fig. 2]), while leftward expression was elevated slightly at the basal level and more pro-

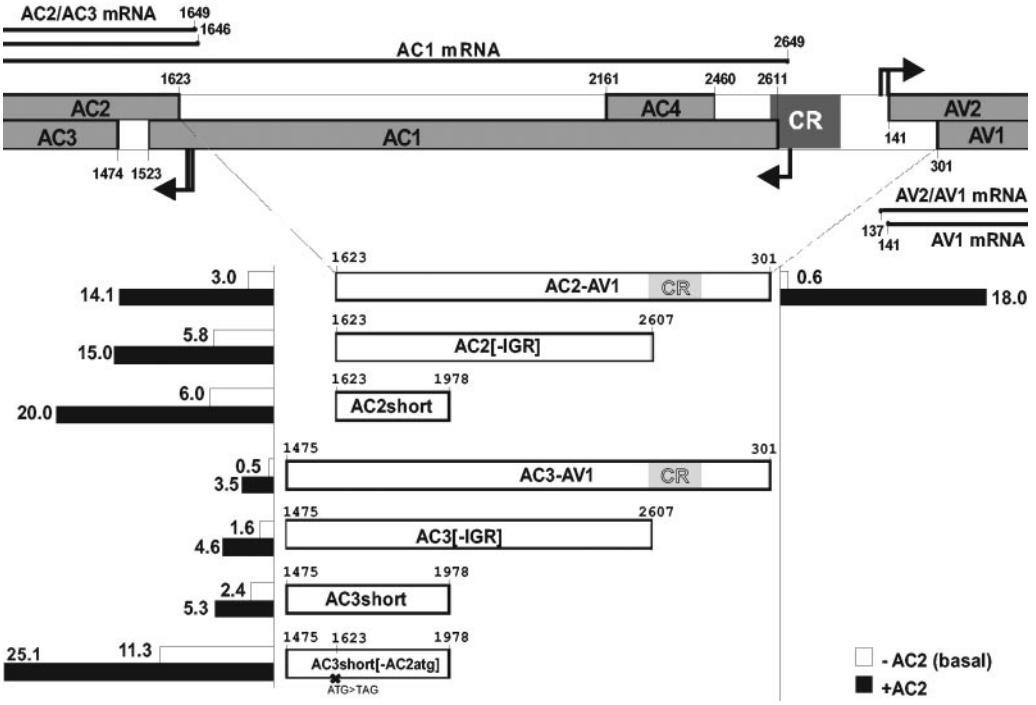

FIG. 3. Mapping of the monodirectional promoter driving the AC2/3 transcription unit. A portion of MYMV DNA-A is represented schematically. The promoter segments tested in *N. plumbaginifolia* protoplasts are shown below the scheme, and the relative expression levels in the leftward and rightward directions are indicated. Annotation are as in Fig. 2.

nouncedly at the AC2-mediated level (Fig. 2). These results show that the BC1 and BV1 promoters and AC2-responsive elements of DNA-B are located outside of the CR. To further map the DNA-B promoters, shorter segments from each AUG start codon to the CR border were tested. Although the basal level of expression driven by BC1short did not change, its response to AC2 dropped dramatically (Fig. 2). In contrast, BV1short was even more strongly induced by AC2 than the longer version, although its basal activity was unchanged. These results suggest that the main AC2-responsive element on DNA-B is shared between the leftward and rightward promoters and is located within a 390-bp noncoding region between CR and the BV1 ORF.

The begomovirus AC1 protein has been shown to repress transcription driven by its own promoter (9, 13, 16, 17, 24, 51). Consistent with this, expression of MYMV AC1 from a separate plasmid driven by the 35S promoter led to a fivefold decrease in leftward expression from both AC1–AV2 and AC1–AV1 promoter segments, while basal rightward expression was unaffected (data not shown). When both AC1 and AC2 proteins were coexpressed from the corresponding plasmids in a 1:1 ratio, leftward expression decreased about threefold for both promoter segments (Fig. 2, DNA-A, gray bars), indicating that AC2 is unable to alleviate the repressive effect of AC1. Strikingly, rightward expression from both the AV2 and AV1 start codons was synergistically enhanced by the combination of AC2 and AC1 (Fig. 2, DNA-A).

An additional, monodirectional MYMV promoter. A 1,407-bp segment of MYMV DNA-A spanning the sequences from AV1 to the AC2 start codon was fused to the CAT reporter and tested for promoter activity in the protoplast system. The resulting basal CAT expression level was twice that of the AC1 promoter and could be further transactivated by AC2 (4.6-fold), thus reaching 14.1% of the control 35S promoter activity (Fig. 3). To test the effect of extra viral sequences on expression in the rightward direction, the CAT reporter was also fused to the AV1 start codon. In this case, both basal and AC2-mediated expression levels were proportionally increased (Fig. 3) compared to the shorter versions of the rightward promoter (AC1–AV1 and AC4–AV1 [Fig. 2]). This suggests that an additional enhancer element contributing to rightward transcription is located between the AC2 and AC4 start codons. An alternative interpretation would be that the C-terminally truncated AC1 protein, which can potentially be expressed from this construct, may exert a positive effect on the rightward promoter, as was observed above for full-length AC1 expressed from a separate construct. However, as this truncated protein is driven by the weak AC1 promoter, it may not accumulate to sufficient levels in our transient system.

To test the significance of IGR-based promoter elements for AC2 expression, the entire IGR or a larger fragment was deleted (yielding AC2[-IGR] and AC2short, respectively). Both these deletions resulted in a roughly twofold increase in basal expression (Fig. 3), showing that the remaining sequences upstream of the AC2 start codon include an autonomous promoter. Notably, both longer and shorter versions of the AC2 promoter were transactivated by AC2. Taken together these results reveal a strong promoter, which can be significantly up-regulated by AC2, within a 346-bp region upstream of the AC2 start codon.

To investigate the AC3 expression strategy, we extended the three versions of the AC2 promoter up to the AC3 start codon

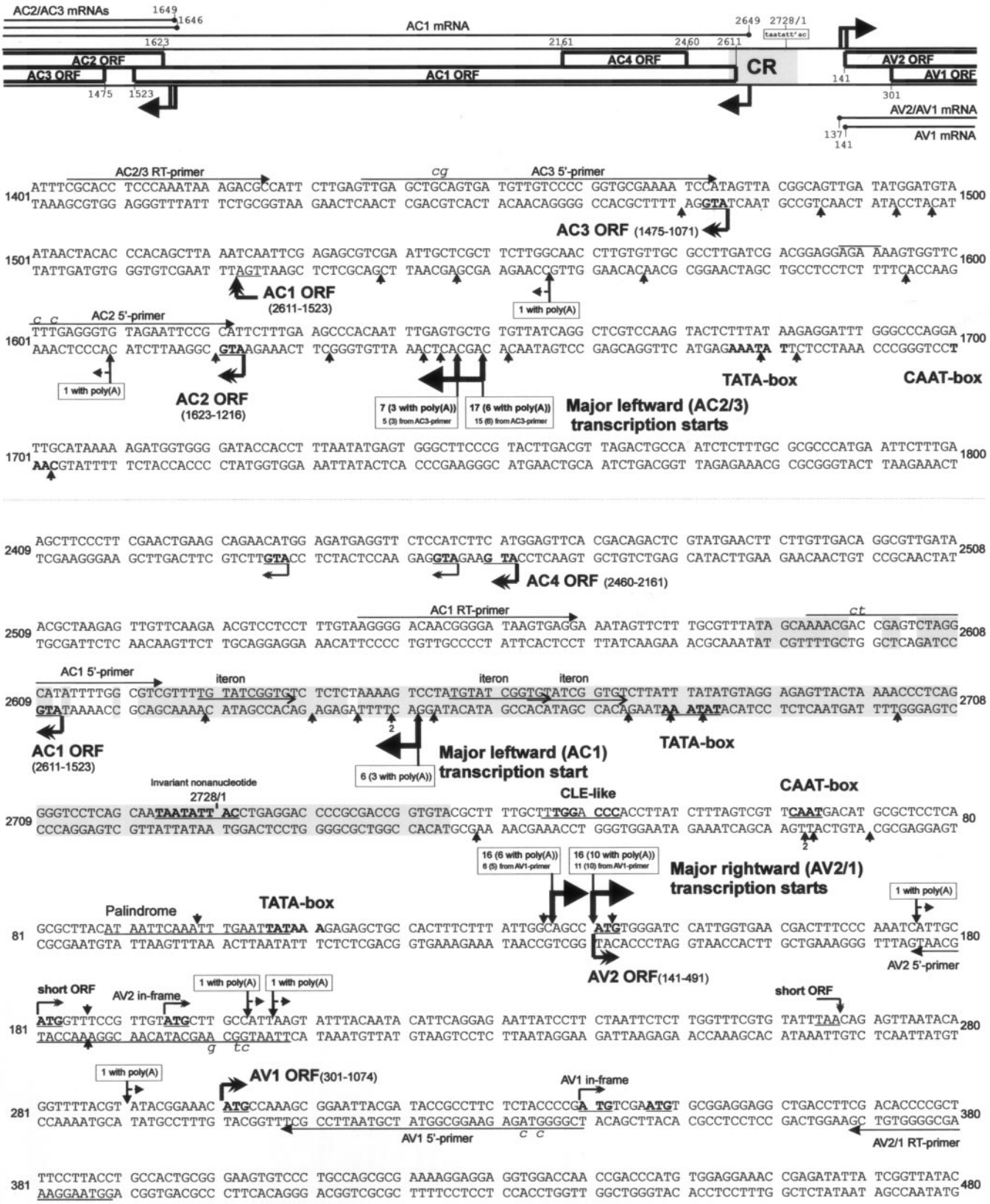
AC2/AC3 mRNAs
AC1 mRNA
AC2 ORF
AC3 ORF
AC1 ORF
AC4 ORF
CR
AV2 ORF
AV1 ORF
AV2/AV1 mRNA
AV1 mRNA
AC2/3 RT-primer
AC3 5'-primer
AC3 ORF (1475-1071)
AC1 ORF (2611-1523)
AC2 5'-primer
AC2 ORF (1623-1216)
TATA-box
CAAT-box
Major leftward (AC2/3) transcription starts
AC4 ORF (2460-2161)
AC1 RT-primer
AC1 5'-primer
iteron
Major leftward (AC1) transcription start
Invariant nonanucleotide
CLE-like
Major rightward (AV2/1) transcription starts
Palindrome
AV2 ORF(141-491)
AV2 5'-primer
short ORF
AV2 in-frame
AV1 ORF(301-1074)
AV1 in-frame
AV1 5'-primer
AV2/1 RT-primer

and fused them to the CAT reporter. All three AC3::CAT constructs yielded expression levels three- to sixfold lower than the corresponding AC2::CAT fusions, both in the absence and in the presence of AC2 protein (Fig. 3). This proportional decrease indicates that AC3 expression is coupled to AC2 expression, such that the former always represents an almost constant fraction of the latter. This implies leaky scanning translation (reviewed in reference 29), in which a certain fraction of scanning ribosomes bypass the AC2 start codon with its suboptimal (**AGAAUGC**) context and initiate translation at the downstream AC3 AUG start codon with its optimal (**ACUAUGG**) context (the region between the two start codons has no additional AUG). To test this assumption, we mutated the AC2 AUG start codon to UAG (stop codon) in the construct AC3short. The model would predict that ribosomes that normally initiate at the AC2 AUG should now migrate further downstream and contribute to AC3 translation. In good agreement with this prediction, the mutation resulted in an increase of AC3 expression from 2.4% to 11.3% of the control, which is close to the combined levels for the nonmutated AC3short and AC2short constructs (8.4%) (Fig. 3). Moreover, like other versions of AC2 and AC3 fusions, the mutated AC3short construct was also transactivated by AC2 (~2.5-fold [Fig. 3]). Taken together, the AC2short-promoter appears to drive expression of both AC2 and AC3, and no significant separate AC3-specific promoter activity is required.

Mapping of transcription start sites. To corroborate the above results, we precisely mapped the viral transcripts harvested from the youngest leaves of MYMV-infected blackgram plants using the cRT-PCR method (6). cRT-PCR allows simultaneous mapping of both the transcription start site (cap site) and the polyadenylation site of a given mRNA due to its preferential intramolecular ligation following a decapping step (see Materials and Methods). Authentic viral mRNA sequences amplified by this method usually contained adenine runs of different lengths (up to 75 nt) at the junction between cap and poly(A) sites (see Fig. S1 and S2 in the supplemental material). The MYMV sequence annotated with the primers used, the TATA and CAAT boxes, major and minor transcription start sites, polyadenylation sites, and splice signals are shown in Fig. 4 to 6. Note that, for each transcription unit, 22 to 41 individual positive clones obtained from at least two independent RNA samples were sequenced (see the statistics in Tables S2 and S3 in the supplemental material).

Criteria for "good mRNAs" should be that (i) cRT-PCR yields cDNA fragments with poly(A) stretches, (ii) a cap site is located approximately 31 to 35 nt downstream from a TATA box, and (iii) similar clones are clustered. Fragments adhering to these criteria were obtained for all the major transcription units analyzed (coordinates of sites indicated in the maps in Fig. 2 and 3). However, the yield of high-quality transcripts varied from unit to unit. Generally, high-quality transcripts were more abundant (~50%) for the rightward units AV2/1 and BV1 and the AC2/3 unit and less abundant (10 to 25%) for the leftward units AC1/4 and BC1 (see Table S2 in the supplemental material). This might indicate that the latter transcripts are less stable. Interestingly, while mapping the AC1 transcript, we found many nonpolyadenylated sequences starting upstream of the TATA box (Fig. 4, small arrows). One such upstream start was also found for the rightward AV2/1 transcription unit (Fig. 4). Such RNA sequences may represent breakdown products of readthrough transcription on the circular viral DNA. A pair of such sense and antisense transcripts could lead to formation of the double-stranded RNA that triggers RNA silencing and generation of viral small interfering RNAs (siRNAs). Indeed, we have detected such siRNAs derived from the MYMV promoter region (P. V. Shivaprasad, R. Akbergenov, and M. M. Pooggin, unpublished). Virus-derived siRNA accumulation during normal infection has also been reported for other begomoviruses (4, 31).

The major rightward transcription initiation events on DNA-A were mapped to positions A137 and A141, 31 and 35 nucleotides downstream from a consensus TATA box (TATAAA) (Fig. 4). These events might generate two distinct mRNAs, both of which could be used for translation of the AV1 ORF (starting from A301) but only the first for translation of the AV2 ORF (starting from A141), since the shorter species would lack the necessary leader required for translation of AV2 (see Discussion).

For the leftward AC1 transcription unit, a single major start site was detected at position 2649, at a proper distance from a consensus TATA box (Fig. 4). Because of only very low levels of CAT expression from the AC4 start codon, we did not attempt to map a separate AC4 transcription unit. Moreover, the AC1 transcript originating from the major leftward site could serve as a dicistronic mRNA for both the AC1 and AC4 proteins.

Using AC3 ORF-specific primers for cRT-PCR, two major closely located transcription start sites were mapped 23 and 26 nt upstream of the AC2 start codon and at an optimal distance from a consensus TATA box located further upstream (Fig. 4). This confirms the finding of an autonomous AC2 promoter discussed above. In addition, two minor clones associated with poly(A) stretches were found between the AC2 and AC3 ATG codons (Fig. 4). We cannot distinguish whether the latter are derived from breakdown products or represent true minor initiation sites. In any case, those two sites would not be properly spaced downstream of the consensus TATA box. As described above, AC3 is most likely expressed as a second cistron from

FIG. 4. Mapping of the DNA-A transcription start sites. A portion of MYMV DNA-A is represented schematically, with the major transcription start sites (thick bent arrows) and corresponding transcripts (capped lines) depicted together with their genomic positions. The nucleotide sequence below is that of the viral and complementary strands encoding the rightward (AV2 and AV1) and leftward (AC1, AC4, AC2, AC3) ORFs, respectively; start and stop codons of the long and short ORFs are indicated by bent arrows with double arrowheads. Small vertical arrows above the viral strand and below the complementary strand indicate 5′ termini of cDNA sequences amplified by cRT-PCR (the respective RT- and ORF-specific 5′ primers used are indicated on the sequence by long, thin horizontal arrows). The number of clones determining each major start site and those associated with poly(A) stretches are given in boxes. The CR nucleotides identical in DNA-A and DNA-B are highlighted (gray background), and the three 11-nt iterons are shown by arrows between the strands. The nucleotide numbering of the circular viral genome begins with and ends at the nick site on the invariant nonanucleotide (boldfaced and underlined) in the CR.

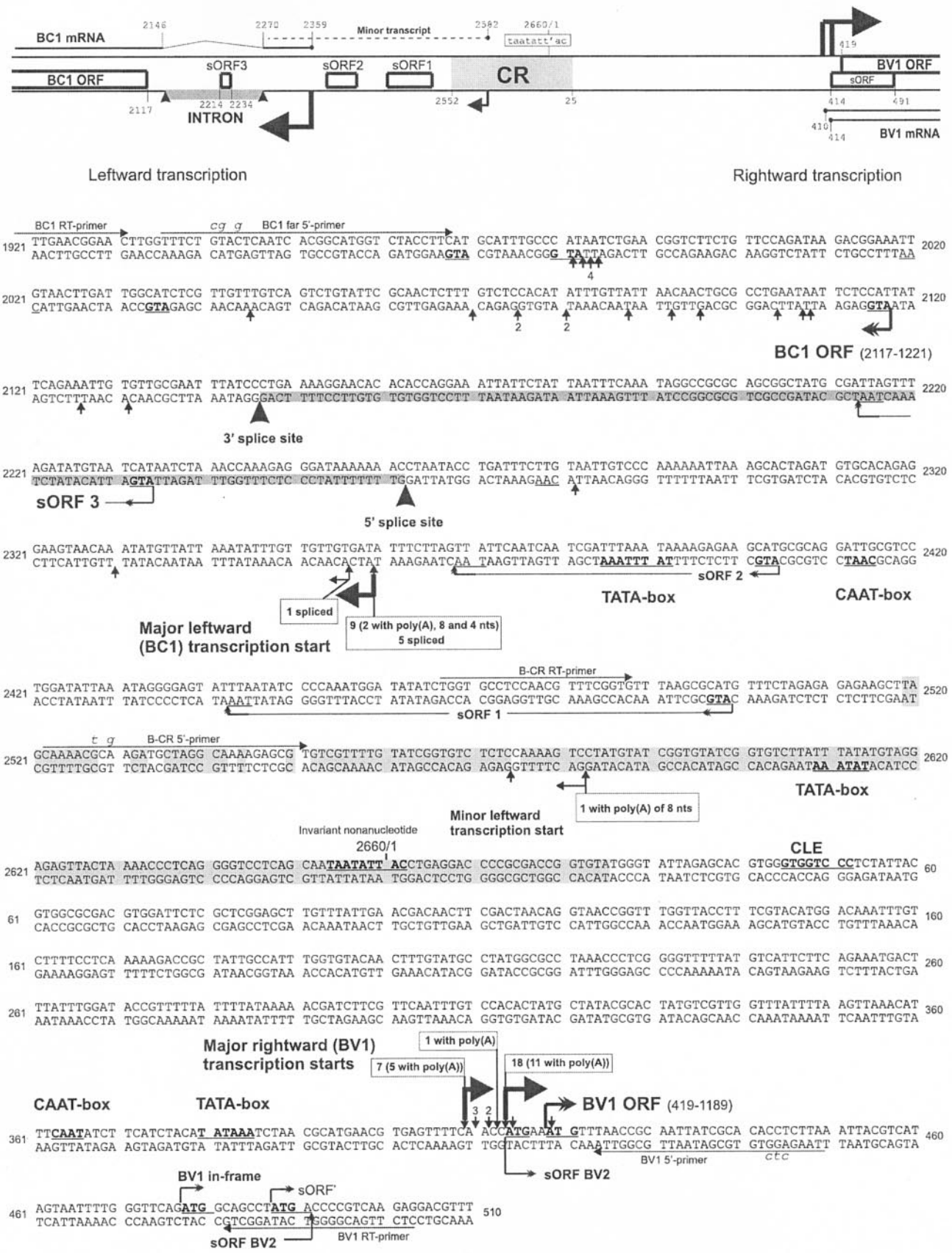
BC1 mRNA
Minor transcript
BC1 ORF
sORF3
sORF2
sORF1
CR
INTRON
BV1 ORF
sORF
BV1 mRNA
Leftward transcription
Rightward transcription
BC1 RT-primer
BC1 far 5'-primer
BC1 ORF (2117-1221)
3' splice site
sORF 3
5' splice site
sORF 2
TATA-box
CAAT-box
1 spliced
9 (2 with poly(A), 8 and 4 nts)
5 spliced
Major leftward
(BC1) transcription start
B-CR RT-primer
sORF 1
B-CR 5'-primer
TATA-box
1 with poly(A) of 8 nts
Minor leftward
transcription start
Invariant nonanucleotide
2660/1
CLE
Major rightward (BV1)
transcription starts
1 with poly(A)
7 (5 with poly(A))
18 (11 with poly(A))
CAAT-box
TATA-box
BV1 ORF (419-1189)
BV1 5'-primer
sORF BV2
BV1 in-frame
sORF'
sORF BV2
BV1 RT-primer

the major transcription unit driven by the strong AC2 promoter.

The two major BV1 transcription start sites were mapped to A410 and A414 (Fig. 5), at an optimal distance from a consensus TATA box and a few bases upstream of the BV1 AUG start codon (at A419). Interestingly, the latter is preceded by another AUG, which creates a short ORF (sORF) (hereafter called BV2) overlapping the BV1 ORF; the first nucleotide of BV2 (A410) coincides with the second major transcription start site (Fig. 5). A similar overlapping sORF occurs in most isolates of MYMV, in the closely related *Mungbean yellow mosaic India virus* (MYMIV), and in some other, though not all, begomoviruses (not shown). This is strikingly reminiscent of the above-described finding that the AV2 AUG coincides with the second rightward transcription start site on DNA-A (Fig. 4). As suggested above, a short leader should allow ribosomes to bypass the first AUG (of sORF BV2) and reach the authentic BV1 start codon.

Consistent with the promoter analysis, the major BC1 transcription start site was detected at position 2359, about 200 bp from the CR (Fig. 5). At an optimal distance of 33 bp upstream of this site, a nonconsensus TATA box, TATTTAAA, was identified using PLACE Web Signal Scan (21; www.dna.affrc.go.jp/htdocs/PLACE). This TATA box is preceded by a consensus CAAT box at position −56. In several, but not all, BC1 clones, including those with and without poly(A) tails, a sequence of 123 nt between positions 2146 and 2270 was missing (see Fig. 5; also see Fig. S2, panel B, in the supplemental material). These results suggest that the BC1 transcript exists in spliced and unspliced forms. Inspection of this region of the MYMV sequence revealed all the characteristic features of a canonical plant intron (30, 44), namely, (i) a consensus 5′ splice site (AG/**GU** [the more conserved dinucleotide is boldfaced]), (ii) a U-rich sequence (41%), and (iii) a consensus 3′ splice site (C**AG**/G [the invariant dinucleotide is boldfaced). The entire 123-nt intron is located within the region between the transcription start site (at nt 2359) and the BC1 AUG start codon (at nt 2117) and contains an sORF of 7 codons (here called sORF3, the last of the three sORFs on the complementary strand between the CR and BC1 ORF [see Fig. 5]).

Sequence alignment of the DNA-B components of five isolates of MYMV-Vig, a distinct strain of MYMV (32), five isolates of the closely related MYMIV, and also *Horsegram yellow mosaic virus* (HYMV) showed that features of both the BC1 promoter and the intron-containing transcription unit are conserved with only a few minor deviations (see Fig. S3 in the supplemental material). Furthermore, in all seven isolates of ACMV, a consensus intron of 239 nt was recognized 40 nt upstream of the BC1 ORF. This intron conservation allowed us to predict a transcription start site preceded by a consensus TATA box for the BC1 transcription unit in ACMV (see Fig. S3 in the supplemental material).

Mapping of poly(A) sites. cRT-PCR also reveals details of RNA processing and polyadenylation (Fig. 6; see also Table S3 in the supplemental material). The poly(A) stretches identified here ranged in length from 4 to 75 nt. For DNA-A rightward transcription, one major poly(A) site at position 1095 was detected, pre-mRNA cleavage in this case having occurred either just upstream or downstream of A1095. This site is located downstream of the AV1 stop codon and at a proper distance of 21/22 nt downstream of the first A (at position 1073) of the consensus poly(A) signal (AAUAAA) that overlaps the double translational stop codon (UAAUAAA). In addition, we found minor poly(A) sites both just upstream and downstream of the major site (Fig. 6).

For the leftward transcription of both the AC1/4 and AC2/3 units, one common major poly(A) site was identified at position 1066, confirming that both AC1 and AC2 promoter-driven transcripts are 3′ coterminal. Here also, minor poly(A) sites were found both upstream and downstream of the major site (Fig. 6). The major leftward poly(A) site is located 5 nt downstream of the AC3 ORF and 21/22 nt downstream of a near-consensus poly(A) signal (AAUACA). Interestingly, the converging rightward and leftward transcription units have their RNA processing signals within their short terminal overlap region of 29 bp (Fig. 6). This is similar to other begomoviruses and reflects the compactness of coding and regulatory information in the viral genome.

3′-end processing of the BV1 transcript was found to be very imprecise (Fig. 6). A total of 12 poly(A) sites were mapped downstream of the BV1 ORF (from position A1191 to G1287), only 2 of which were represented by more than one clone: G1287 (2 clones) and A1223 (3 clones). The latter is located 22 nucleotides downstream of a near-consensus poly(A) signal (AAUAUA). In contrast, a consensus poly(A) signal adjacent to the BV1 stop codon (UAAAAUAAA) did not direct any detectable cleavage at an optimal distance downstream of it.

For the BC1 transcription unit, only three clones associated with poly(A) stretches were identified, which did not allow us to define any major poly(A) site. One poly(A) site for the spliced transcript driven by the major BC1 promoter maps to position 1196, 15 nucleotides downstream of a consensus poly(A) signal (Fig. 6). However, another poly(A) site is located at position 1233, i.e., in front of the BC1 stop codon (at position 1221). 3′ untranslated regions of several nonpolyadenylated spliced or unspliced transcripts terminate behind the BC1 stop codon and scatter over a 140-bp region up to position 1078 (Fig. 6). Taken together, these results suggest that polyadenylation of the leftward transcripts on DNA-B is also imprecise. Furthermore, both leftward and rightward transcripts appear to overlap the small intergenic region between the BV1 and BC1 stop codons and therefore, like the converging transcripts of DNA-A, might also form a double-stranded RNA leading to a silencing response.

Detection of MYMV transcripts by Northern blotting. To validate the cRT-PCR mapping results and gain information on the relative abundances of viral transcripts at early and late stages of infection, we performed Northern blot hybridization

FIG. 5. Mapping of the DNA-B transcription start sites. A portion of MYMV DNA-B, including the large IGR between the leftward (BC1) and rightward (BV1) ORFs, is represented schematically; the major and minor transcription start sites in both directions are indicated (bent arrows) and corresponding transcripts (capped lines) depicted. The corresponding nucleotide sequence is shown below and annotated as in Fig. 4. The intron sequence in the BC1 transcription unit is highlighted and flanked with large arrowheads indicating the spice sites.

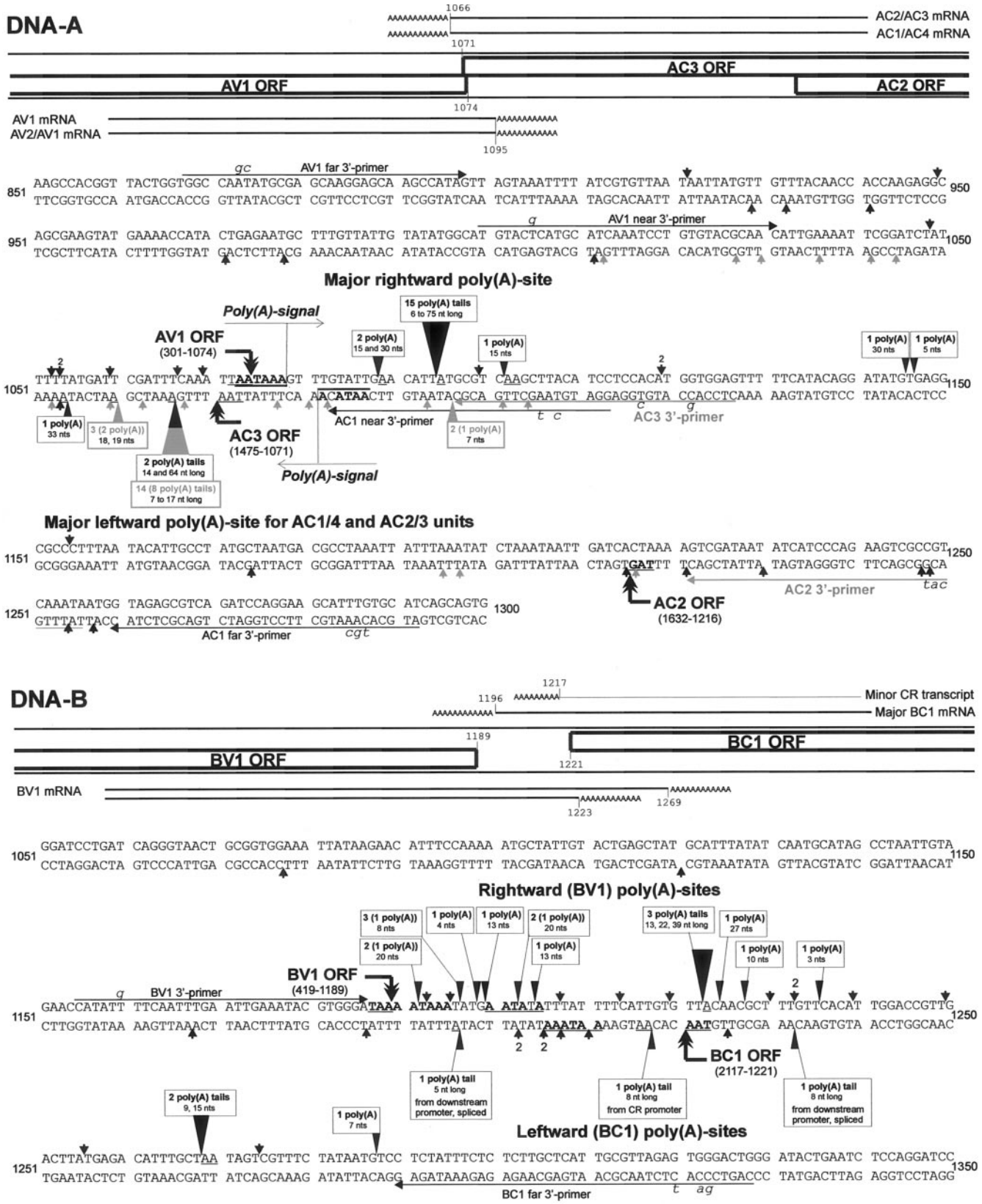
DNA-A
1066
AC2/AC3 mRNA
AC1/AC4 mRNA
1071
AC3 ORF
AV1 ORF
AC2 ORF
1074
AV1 mRNA
AV2/AV1 mRNA
1095
gc
AV1 far 3'-primer
851 AAGCCACGGT TACTGGTGGC CAATATGCGA GCAAGGAGCA AGCCATAGTT AGTAAATTTT ATCGTGTTAA TAATTATGTT GTTTACAACC ACCAAGAGGC 950
TTCGGTGCCA ATGACCACCG GTTATACGCT CGTTCCTCGT TCGGTATCAA TCATTTAAAA TAGCACAATT ATTAATACAA CAAATGTTGG TGGTTCTCCG
g
AV1 near 3'-primer
951 AGCGAAGTAT GAAAACCATA CTGAGAATGC TTTGTTATTG TATATGGCAT GTACTCATGC ATCAAATCCT GTGTACGCAA CATTGAAAAT TCGGATCTAT 1050
TCGCTTCATA CTTTTGGTAT GACTCTTACG AAACAATAAC ATATACCGTA CATGAGTACG TAGTTTAGGA CACATGCGTT GTAACTTTTA AGCCTAGATA
Major rightward poly(A)-site
Poly(A)-signal
15 poly(A) tails
6 to 75 nt long
AV1 ORF
(301-1074)
2 poly(A)
15 and 30 nts
1 poly(A)
15 nts
1 poly(A)
30 nts
1 poly(A)
5 nts
1051 TTTTATGATT CGATTTCAAA TTAATAAAGT TTGTATTGAA CATTATGCGT CAAGCTTACA TCCTCCACAT GGTGGAGTTT TTCATACAGG ATATGTGAGG 1150
AAAATACTAA GCTAAAGTTT AATTATTTCA AACATAACTT GTAATACGCA GTTCGAATGT AGGAGGTGTA CCACCTCAAA AAGTATGTCC TATACACTCC
1 poly(A)
33 nts
3 (2 poly(A))
18, 19 nts
AC3 ORF
(1475-1071)
AC1 near 3'-primer
2 (1 poly(A)
7 nts
AC3 3'-primer
2 poly(A) tails
14 and 64 nt long
14 (8 poly(A) tails)
7 to 17 nt long
Poly(A)-signal
Major leftward poly(A)-site for AC1/4 and AC2/3 units
1151 CGCCCTTTAA TACATTGCCT ATGCTAATGA CGCCTAAATT ATTTAAATAT CTAAATAATT GATCACTAAA AGTCGATAAT ATCATCCCAG AAGTCGCCGT 1250
GCGGGAAATT ATGTAACGGA TACGATTACT GCGGATTTAA TAAATTTATA GATTTATTAA CTAGTGATTT TCAGCTATTA TAGTAGGGTC TTCAGCGGCA
AC2 3'-primer
tac
AC2 ORF
(1632-1216)
1251 CAAATAATGG TAGAGCGTCA GATCCAGGAA GCATTTGTGC ATCAGCAGTG 1300
GTTTATTACC ATCTCGCAGT CTAGGTCCTT CGTAAACACG TAGTCGTCAC
AC1 far 3'-primer
cgt
DNA-B
1217
1196
Minor CR transcript
Major BC1 mRNA
1189
BC1 ORF
BV1 ORF
1221
BV1 mRNA
1223
1269
1051 GGATCCTGAT CAGGGTAACT GCGGTGGAAA TTATAAGAAC ATTTCCAAAA ATGCTATTGT ACTGAGCTAT GCATTTATAT CAATGCATAG CCTAATTGTA 1150
CCTAGGACTA GTCCCATTGA CGCCACCTTT AATATTCTTG TAAAGGTTTT TACGATAACA TGACTCGATA CGTAAATATA GTTACGTATC GGATTAACAT
Rightward (BV1) poly(A)-sites
3 (1 poly(A))
8 nts
1 poly(A)
4 nts
1 poly(A)
13 nts
2 (1 poly(A))
20 nts
3 poly(A) tails
13, 22, 39 nt long
1 poly(A)
27 nts
2 (1 poly(A))
20 nts
1 poly(A)
13 nts
1 poly(A)
10 nts
1 poly(A)
3 nts
BV1 ORF
(419-1189)
g
BV1 3'-primer
1151 GAACCATATT TTCAATTTGA ATTGAAATAC GTGGGATAAA ATAAATATGA ATATATTTAT TTTCATTGTG TTACAACGCT TTGTTCACAT TGGACCGTTG 1250
CTTGGTATAA AAGTTAAACT TAACTTTATG CACCCTATTT TATTTATACT TATATAAATA AAAGTAACAC AATGTTGCGA AACAAGTGTA ACCTGGCAAC
BC1 ORF
(2117-1221)
1 poly(A) tail
5 nt long
from downstream
promoter, spliced
1 poly(A) tail
8 nt long
from CR promoter
1 poly(A) tail
8 nt long
from downstream
promoter, spliced
2 poly(A) tails
9, 15 nts
1 poly(A)
7 nts
Leftward (BC1) poly(A)-sites
1251 ACTTATGAGA CATTTGCTAA TAGTCGTTTC TATAATGTCC TCTATTTCTC TCTTGCTCAT TGCGTTAGAG TGGGACTGGG ATACTGAATC TCCAGGATCC 1350
TGAATACTCT GTAAACGATT ATCAGCAAAG ATATTACAGG AGATAAAGAG AGAACGAGTA ACGCAATCTC ACCCTGACCC TATGACTTAG AGGTCCTAGG
BC1 far 3'-primer
t ag

analysis of total RNAs isolated from two parts of MYMV-infected blackgram seedlings: (i) the uppermost unopened leaf buds, which should contain a high proportion of the virus at early stages of its replication cycle (Fig. 7, sample 2), and (ii) newly opened young leaves, in which the products of late viral genes should start to accumulate (Fig. 7, sample 3). Five MYMV-specific DNA probes were derived from the complete coding regions of the AC1, AC2, AV1, BC1, and BV1 genes, respectively (Fig. 7).

The results revealed that viral transcripts corresponding to all the five transcription units mapped by cRT-PCR accumulate in infected plants. The approximate sizes of the major transcripts, calculated based on the positions of the RNA markers (2.37 kb, 1.35 kb, and 0.24 kb), matched the expected sizes, taking into account variations in poly(A) tail length (up to and probably beyond the longest tail of 75 nt that we have cloned). As expected, the 1.65-kb AC1/4 transcript is detected by both the AC1 and AC2 probes, the 0.65-kb AC2/3 transcript by the AC2 probe, the 1.0-kb AV2/1 transcript by the AV1 probe, the 0.9-kb BV1 transcript by the BV1 probe, and the 1.1-kb spliced BC1 transcript by the BC1 probe (Fig. 7). By using the BC1 probe, three additional, less abundant transcripts of ~0.7 kb, ~1.2 kb, and ~1.4 kb were also detected. The ~1.2-kb transcript (Fig. 7, pre-BC1) is likely to be an unspliced version of the major BC1 transcript, as it was also detected by cRT-PCR (see Fig. S2 and Table S2 in the supplemental material). The ~1.4-kb transcript (Fig. 7, CR) might originate from the DNA-B CR, consistent with a minor transcription start site being mapped to this region (see Fig. S2 and Table S2 in the supplemental material). The nature of the third minor band (Fig. 7, double asterisk) will require further investigation. Likewise, an additional transcript of ~1.4 kb detected by the AC2 probe (Fig. 7, single asterisk) remains to be investigated. The fact that this transcript does not significantly hybridize to the AC1 probe suggests that it may be a readthrough version of the AC2/3 transcript. Consistent with this interpretation is the cloning of several RNA sequences partially or fully overlapping the DNA-A IGR (see Fig. 4; also see Table S2 in the supplemental material), which could result from processing of a leftward readthrough transcript followed by partial degradation of its 3′ portion spanning the IGR.

Interestingly, the relative abundances of viral transcripts in the younger and older tissues (Fig. 7; compare samples 2 and 3) correlate well with the activities of the corresponding promoters in the absence and presence of AC2, as observed in plant protoplasts (see Fig. 2 and 3). At the early stages of infection (sample 2), the transcripts for the AV2/1, BV1, and BC1 genes are much less abundant than at the later stages (sample 3), confirming the AC2-inducible nature of their promoters. In contrast, the AC2/3 transcript accumulated to high levels in both samples, reflecting the constitutive nature of its promoter, as observed in the protoplast system. Furthermore, accumulation of the AC1/4 transcript is low in both samples, consistent with the low basal activity of the AC1 promoter and the negative-feedback regulation even in the presence of AC2. Finally, the relatively high accumulation of the AV2/1 transcript early in infection could be due to a synergistic positive effect of AC1 protein on AC2-mediated activation of the AV2/1 promoter.

Besides the above-mentioned long transcripts, smears in the bottom parts of the blots were observed, which most likely represent degradation intermediates of the respective major transcripts. Notably, in the case of the AC2/3 transcript, these degradation products accumulate equally in both samples to rather high levels, indicating that this early transcript might be a major target of the antiviral defense based on RNA silencing. Consistent with this notion, an AC2 gene region was found to be a hot spot for begomovirus small RNAs of ~21 to 24 nt, the hallmarks of RNA silencing (56; R. Akbergenov and M. M. Pooggin, unpublished).

DISCUSSION

Viruses in general, and plant geminiviruses in particular, economize the signals required for expression of their genomes. In order to minimize genome size, enhancer elements can be shared by different promoters, promoters can extend into and/or be contained entirely within protein coding regions, multiple (alternatively) spliced and overlapping transcripts can be created, and transcripts can be polycistronic or encode polyprotein precursors giving rise to several individual proteins upon processing. Our study reveals that, with the exception of polyproteins (which have not been found in geminiviruses), most of these strategies are used by MYMV, and characterizes some new features of regulation of begomovirus gene expression.

Transcriptional control in *cis* and in *trans*. The five major MYMV transcription units mapped and characterized here confirm that, like other geminiviruses, MYMV has evolved a bidirectional mode of transcription, with the bidirectional promoter of DNA-A contained within the 252-bp IGR between the AC1 and AV2 start codons and the bidirectional promoter of DNA-B contained within a larger IGR (957 bp) between the BC1 and BV1 start codons. These bidirectional promoters direct production of two transcripts from each DNA: AC1/4, AV2/1, BC1, and BV1. A fifth major transcript is driven by an additional, monodirectional AC2 promoter (see Fig. 1 and 7). The bidirectional promoters contain separate, direction-specific core elements located at an optimal distance from their respective transcription start sites. Since enhancer elements can act bidirectionally (see, e.g., reference 59), they could be shared by the core promoters. Indeed, both rightward and leftward expression is transactivated by the viral transcription factor AC2, and in the case of DNA-B, we could show that an

FIG. 6. Mapping of polyadenylation sites on DNA-A and DNA-B. Schematic representations of the DNA-A and DNA-B regions with converging ORFs and polyadenylated transcripts. The nucleotide sequences of the viral and complementary strands (below each scheme) are annotated with the major and minor poly(A) sites [large and small filled triangles, respectively, together with boxes noting the number of cRT-PCR clones polyadenylated at that position and the range of lengths of the poly(A) stretch] for both rightward (above the viral strand) and leftward (below the complementary strand) transcription units. Small vertical arrows indicate 3′ termini of other nonpolyadenylated cDNAs. The 3′ primers for cRT-PCR are shown along the sequence by horizontal arrows.

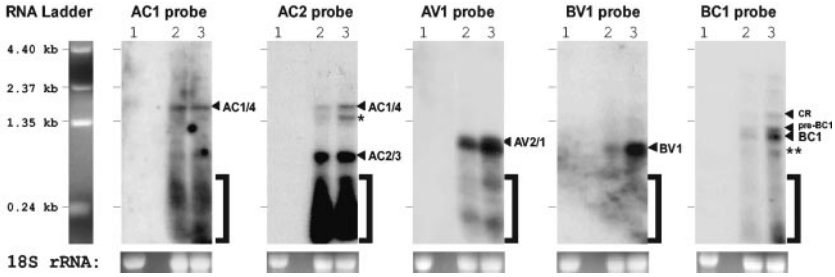

FIG. 7. Detection of MYMV transcripts in infected plants by Northern blot hybridization. Three samples of total RNA, one from healthy (lanes 1) and two from MYMV-infected (lanes 2 and 3) blackgram plants, were separated on five gels, blotted, and hybridized with five different probes (AC1, AC2, AV1, BV1, and BC1, respectively). The lane numbers correspond to the sample numbers. Positions of the RNA markers (4.4 kb to 0.24 kb; shown on the left) are indicated on each blot. As a loading control, ethidium bromide-stained 18S rRNA is shown below each blot. The major viral transcripts, whose sizes correspond to those deduced from the cRT-PCR mapping results, are indicated by arrowheads. Two additional hybridization signals are shown by asterisks. Hybridization smears in the bottom portions of the blots (indicated by brackets) represent degradation intermediates of the corresponding major transcripts.

AC2-responsive region is indeed shared between the rightward and leftward promoters. However, the degree of AC2-mediated activation differs: it is considerable (~15- to 300-fold) for the "late" promoters driving the AV1/2, BV1, and BC1 units but much less pronounced (~3- to 5-fold) for the "early" promoters driving the AC1/4 and AC2/3 units. On both the A and B components, basal rightward expression is much lower and is more markedly activated by AC2 than leftward expression.

The basal and activated RNA production profiles in MYMV reflect the need for AC1 protein as an early function, but only in the catalytic quantities required for genome replication, whereas AV1, BC1, and BV1, as structural proteins, are required later and in higher quantities. Indeed, our results show that the AC1 promoter is the weakest of the viral promoters. It is moderately transactivated by AC2 but downregulated by AC1, even in the presence of AC2 (Fig. 2). Consistently, the AC1/4 transcript driven by this promoter accumulates to relatively low levels at both early and late stages of infection (Fig. 7). Low basal activity of the AC1 promoter in protoplasts was also found for ACMV (13, 24, 60), with transactivation by AC2 protein reported by Frey et al. (13) but not detected by others (17, 24). Although not transactivated by AC2 (9, 51), the TGMV AC1 promoter exhibited a much higher basal activity (9) than MYMV or ACMV. Interestingly, the repressive effect of the AC1 protein was much more pronounced in TGMV (9) than in ACMV (17, 24) and MYMV (this work), possibly reflecting a difference in expression strategies between New World (TGMV) and Old World (ACMV and MYMV) begomoviruses. This difference is further illustrated by the low basal activity and AC2 inducibility of the BC1 promoter observed here for MYMV and earlier for ACMV (13), but not for TGMV (9).

As a key activator of viral transcription, AC2 protein is also expected to be produced early. In fact, the MYMV AC2/3 transcript is the most abundant species in early infection. Production of AC2 protein in large quantities might reflect its role not only in transcriptional activation of late viral genes (47) but also in other activities such as suppression of silencing (55, 56, 58).

A separate transcript covering the AC2 and AC3 genes has been precisely mapped in both monopartite (TLCV) (34) and bipartite (AbMV [14] and TGMV [18, 50]) begomoviruses. However for TGMV, in addition to that transcript, a complex pattern of longer leftward transcripts was detected (18, 50). This, together with a transgenic plant study (19), suggested alternative mechanisms for AC2 and AC3 expression, including translation of AC1, AC2, and AC3 from a single polycistronic RNA (19). Our results for MYMV argue against this latter hypothesis, because of the presence of a precisely mapped and highly abundant separate AC2/3 transcript driven by the strong promoter located just upstream of the AC2 ORF. It is rather unlikely that the AC2 and AC3 proteins would be alternatively translated by internal initiation from the polycistronic AC1/4 transcript, which accumulates to much lower levels (Fig. 7). Also in ACMV, a similar promoter activity was detected in a short segment upstream of the AC2 ORF, although in that case its activity was only 40% of that of the AC1 promoter (60).

Recently, minichromosomes of AbMV have been fine-mapped and shown to be composed of 11 to 13 nucleosomes (37). Those associated with 11 or 12 nucleosomes have open gaps, which might be accessible for interaction with host replication and transcription factors. Accordingly, on both DNA-A and DNA-B these gaps occur in the IGR, which contain the CR-based origin of replication and the bidirectional promoters. One additional gap maps upstream of the AC2 ORF (37), thus coinciding with the promoter region mapped here for the AC2/3 transcription unit.

Our data also suggest that an enhancer element(s) of the strong AC2 promoter might also act on the bidirectional promoter located in the IGR. Indeed, both basal and AC2-mediated expression from the AV1 start codon was increased by addition of the sequence between the AC2 and AC4 start codons. Conversely, the bidirectional IGR-based promoter seems to have a negative effect on basal expression driven by the AC2 promoter, although this effect is almost completely alleviated in *trans* by the AC2 gene product (Fig. 3). Interestingly, a similar negative effect of the CR-based core promoter on downstream leftward transcription is also observed on DNA-B (Fig. 2).

Upstream leftward transcription from the bidirectional promoter might inhibit downstream AC2 promoter activity by occluding binding sites for transcription factors and/or displacing such factors. This would imply that strong constitutive expression from the AC1 promoter would not be compatible with efficient expression of AC2 driven by the downstream AC2

promoter. In this regard, the negative-feedback regulation of the AC1 promoter by AC1 protein might be necessary to maintain high expression of AC2.

The negative effect of MYMV AC1 on its own leftward promoter contrasts with its positive effect on rightward transcription exerted via synergistic cooperation with AC2 (Fig. 2), i.e., AC1 appears to divert DNA-A transcription from the leftward to the rightward direction. This is most likely achieved through AC1 binding to the iterons located between the AC1 promoter TATA box and transcription start sites, as demonstrated for TGMV (9, 11, 12), thereby blocking leftward transcription and freeing enhancer elements for rightward transcription. Such synergistic activation of rightward expression by AC1 has not been detected in other begomoviruses to date (13, 16). However, in *Wheat dwarf mastrevirus*, the C1::C2 fusion protein was implicated in activation of the rightward promoter (22), and in that case it appears to require the unfused C1 protein for full activation (5).

Consistent with our hypothesis, AC2-mediated expression from the AC2 promoter or DNA-B promoters was not influenced significantly by AC1 (P. V. Shivaprasad and D. Trinks, unpublished), apparently because these promoters are located outside of the CR, which contains the AC1-binding site. The positive effect of AC1 on transcription from the AV2/1 promoter cannot be explained by an AC1-mediated amplification of the DNA template in our transient system. Otherwise, a similar effect would also have been observed for the full-length DNA-B promoter constructs, which contain the same CR-based origin of replication.

The molecular mechanism of AC2 action at the transcriptional level (47) remains unknown. A conserved late element (CLE) sequence has previously been implicated in AC2-mediated transactivation based on its conservation in begomoviruses (2) and some experimental evidence (40). Our inspection of the MYMV sequence revealed a consensus CLE (GTGGT CCC) at position 45 of DNA-B, 20 bp from CR (Fig. 5), i.e., in the rightward promoter, the most AC2-responsive viral promoter mapped here. In the corresponding region of DNA-A, a sequence deviating from CLE in two positions (TTGGACCC) was also found (Fig. 4). In TGMV, however, a consensus CLE in the DNA-A rightward promoter does not appear to be necessary for transactivation, despite being an integral part of the AC2-responsive module (49). Moreover, the rightward promoters of BGMV DNA-A and DNA-B, being highly responsive to AC2 from BGMV and TGMV, both lack a CLE (25). Further dissection of the structural organization of AC2-responsive promoters will be required to define the contribution of different *cis*-acting elements.

Multiple transcription initiation and polyadenylation sites. In all the transcription units mapped here except AC1 and BC1, transcription initiates at two major closely spaced start sites, 3 to 4 nucleotides apart, within the context CANNN(N)CA, where both adenines are cap sites. Interestingly, this correlates with the presence of a CAAT box in the core promoter. Different transcript variants may serve different functions and/or be differentially regulated. In related situations for the AV1 and BV1 units, the longer transcripts would allow translation from the medium-sized ORF AV2 and sORF BV2, which start in front of and overlap the main ORF, respectively. In both cases translation from the main ORFs (AV1 and BV1) would be inhibited unless leaky scanning occurs. The shorter versions would allow translation only of AV1 (see below) and BV1, respectively, because in both cases the cap site coincides with the first nucleotide of the upstream start codon.

For the BC1 transcription unit, two initiation sites were mapped. The minor initiation event, apparently driven by the CR-based core promoter, would result in a long transcript with originally three leader-based sORFs, while the major downstream initiation event produces a shorter transcript with only one leader-based sORF located in the intron. It can be assumed that these two transcripts are translated with different efficiencies and/or are differentially regulated, as sORFs have been implicated in many types of translational control (33, 41).

For most MYMV transcription units, multiple polyadenylation sites were mapped (Fig. 6). Besides the major poly(A) sites, located at an optimal distance of about 22 nucleotides from consensus or near-consensus poly(A) signals on both DNA components, multiple minor sites were detected upstream and downstream. In this regard, the BV1 unit represents an extreme case, with 12 poly(A) sites scattered over 100 bases downstream of the translation stop codon. The biological significance of such imprecise processing of viral transcripts is unclear, but multiple polyadenylation events are common in plants (39).

Translation initiation by leaky scanning. Neither separate promoters nor separate transcripts have been found for the AC4, AV1, and AC3 genes. Our artificial promoter fragments AV2–AC4 and AV1–AC4 gave rise to only very low expression from the AC4 start codon, even in the presence of AC2. This is in contrast to ACMV, in which relatively high basal expression was observed from the first AUG of AC4 (24). We assume that the leftward MYMV transcript originating from DNA-A CR is polycistronic, allowing direct translation of AC1 and translation of AC4 by leaky scanning. Leaky scanning (reviewed in reference 29) would be favored by the suboptimal initiation context of the AC1 start codon (**A**AU**AUG**C) and the absence of AUG codons between the AC1 and AC4 start codons.

Leaky scanning also seems to be the translation mechanism for AV1 and BV1, the main products of the AV2/1 and BV2/1 transcripts, allowing bypass of the 5′-proximal (AV2 and BV2) AUG start codons due to the suboptimal length of the leaders preceding those AUGs. Even in the longer versions of those transcripts, the leader length of 4 nucleotides is below the critical length of 7 nucleotides determined by Kozak (28). In the case of the AV2/1 unit, downstream translation is further complicated by the presence of two additional AUGs in the region between the AV2 and AV1 start codons, the first creating an sORF and the second being in frame with the AV2 ORF (see Fig. 4). After primary translation of such sORFs, efficient reinitiation of translation is possible (reviewed in references 29 and 41). Similar structural organization of the AV2/1 unit has been reported for ACMV (13, 54) and TLCV (34). Notably, expression levels from the MYMV AV1 and AV2 start codons were comparable, and both responded similarly to the regulatory proteins AC2 and AC1 (Fig. 2), further supporting the notion that these overlapping genes are expressed from the same transcription unit via a coupled mechanism such as leaky scanning.

Several lines of evidence indicate that AC3 is also translated

by leaky scanning from a dicistronic AC2/3 transcript. Firstly, this transcript is highly abundant and driven by the strong AC2 promoter. Secondly, cRT-PCR with AC3 ORF-specific primers did not reveal any major transcription start between the AC2 and AC3 start codons or any splicing event removing the upstream AC2 AUG. Thirdly, transient expression experiments showed that AC3 expression positively correlates with, and always constitutes a constant fraction of, AC2 expression. Fourthly, point mutation of the AC2 start codon increases expression from the AC3 AUG, consistent with the predictions of a leaky scanning model. Finally, inspection of the sequence between the mapped or putative transcription start sites and the AC3 AUG start codon in MYMV, ACMV (all strains but KE), AbMV, TLCV, and TGMV reveals no other AUG codon except the AC2 start codon, which is in a suboptimal moderate context, while the AC3 start codon itself is in the optimal context (Fig. 4 and data not shown).

Taken together, all the evidence suggests that leaky scanning is a major strategy employed by MYMV and, most likely, by other begomoviruses to translate their polycistronic transcription units.

Splicing. Splicing in geminiviruses was first discovered in monopartite geminiviruses of the genus *Mastrevirus*, where it appears to be the only mechanism of expression for the C2 ORF, which lacks its own AUG start codon (1, 43). To our knowledge, splicing has never previously been reported in begomoviruses. Here we provide evidence for a distinct splicing event as part of the expression strategy of MYMV. The 123-nt intron within the BC1 transcription unit appears to be a canonical plant intron processed by the major U2 spliceosome (30, 44). But, unlike most plant introns, it is contained within the leader region preceding the main ORF. The splicing event removes the leader-based sORF, whereby translation efficiency is expected to increase while the coding sequence remains unaltered. Besides removing inhibitory sequences from the BC1 mRNA leader, the splicing process itself might increase the efficiency of BC1 expression by accelerating viral mRNA transport to the cytoplasm for productive translation.

An intron with consensus 5′ and 3′ splice sites and one or more sORFs appears at the same or a nearby location in all isolates of MYMV and MYMIV, as well as in more distantly related begomoviruses including HYMV and ACMV (see Fig. S3 in the supplemental material). In the latter case, the predicted intron is burdened with as many as 6 AUGs (depending on the strain), while the putative leader of the spliced transcript lacks any AUG. The observation that the minor (1.35-kb) and major (1.1-kb) leftward transcripts of ACMV DNA-B (54) are 5′ coterminal (unpublished data discussed in reference 7) may well be explained as a precursor-product relationship consistent with a splicing event removing the 239-nt intron predicted here. In contrast, for *East African cassava mosaic virus*, *South African cassava mosaic virus*, TGMV, and AbMV, inspection of the complementary stand upstream of the BC1 ORF did not reveal any canonical intron, suggesting that the splicing event discovered here for MYMV may not be conserved in all begomoviruses.

Conclusions. In summary, the following new features, which might also apply to other begomoviruses, were revealed for MYMV. The leftward and rightward promoters on DNA-B share the transcription activator AC2-responsive region, which does not overlap with the CR. The transcription unit for BC1 includes a conserved, leader-based intron. Besides negative-feedback regulation of its own leftward promoter on DNA-A, the replication protein AC1, in cooperation with AC2, synergistically transactivates the rightward promoter, which drives a dicistronic transcription unit for the coat protein AV1. AC2 and the replication enhancer AC3 are expressed by leaky scanning from a single dicistronic and highly abundant transcript driven by a strong promoter mapped within the upstream AC1 gene.

ACKNOWLEDGMENTS

We are grateful to Helen Rothnie and Johannes Fütterer for critical reading of the manuscript and to Monika Fasler and Matthias Müller for protoplasting. Special thanks to Thomas Boller and Christian Körner for hosting the group at the Institute of Botany, University of Basel.

This work was funded by the Indo-Swiss Collaboration in Biotechnology (ISCB) and the EU network V grant "VIS," by a Swiss National Science Foundation "SCOPES" grant to R.A., and by a fellowship from CSIR (India) to P.V.S.

REFERENCES

1. **Accotto, G. P., J. Donson, and P. M. Mullineaux.** 1989. Mapping of Digitaria streak virus transcripts reveals different RNA species from the same transcription unit. EMBO J. **8:**1033–1039.
2. **Argüello-Astorga, G. R., R. G. Guevara-Gonzalez, L. R. Herrera-Estrella, and R. F. Rivera-Bustamante.** 1994. Geminivirus replication origins have a group-specific organization of iterative elements: a model for replication. Virology **203:**90–100.
3. **Balaji, V., R. Vanitharani, A. S. Karthikeyan, S. Anbalagan, and K. Veluthambi.** 2004. Infectivity analysis of two variable DNA B components of *Mungbean yellow mosaic virus-Vigna* in *Vigna mungo* and *Vigna radiata*. J. Biosci. **29:**297–308.
4. **Chellappan, P., R. Vanitharani, and C. M. Fauquet.** 2004. Short interfering RNA accumulation correlates with host recovery in DNA virus-infected hosts, and gene silencing targets specific viral sequences. J. Virol. **78:**7465–7477.
5. **Collin, S., M. Fernandez-Lobato, P. S. Gooding, P. M. Mullineaux, and C. Fenoll.** 1996. The two nonstructural proteins from wheat dwarf virus involved in viral gene expression and replication are retinoblastoma-binding proteins. Virology **219:**324–329.
6. **Couttet, P., M. Fromont-Racine, D. Steel, R. Pictet, and T. Grange.** 1997. Messenger RNA deadenylylation precedes decapping in mammalian cells. Proc. Natl. Acad. Sci. USA **94:**5628–5633.
7. **Davies, J. W., R. Townsend, and J. Stanley.** 1987. The structure, expression, functions and possible explanation of geminivirus genomes, p. 31–52. *In* T. Hohn and J. Schell (ed.), Plant DNA infectious agents. Springer-Verlag, Vienna, Austria.
8. **Eagle, P. A., and L. Hanley-Bowdoin.** 1997. *cis* elements that contribute to geminivirus transcriptional regulation and the efficiency of DNA replication. J. Virol. **71:**6947–6955.
9. **Eagle, P. A., B. M. Orozco, and L. Hanley-Bowdoin.** 1994. A DNA sequence required for geminivirus replication also mediates transcriptional regulation. Plant Cell **6:**1157–1170.
10. **Fauquet, C. M., D. M. Bisaro, R. W. Briddon, J. K. Brown, B. D. Harrison, E. P. Rybicki, D. C. Stenger, and J. Stanley.** 2003. Revision of taxonomic criteria for species demarcation in the family *Geminiviridae*, and an updated list of begomovirus species. Arch. Virol. **148:**405–421.
11. **Fontes, E. P., P. A. Eagle, P. S. Sipe, V. A. Luckow, and L. Hanley-Bowdoin.** 1994. Interaction between a geminivirus replication protein and origin DNA is essential for viral replication. J. Biol. Chem. **269:**8459–8465.
12. **Fontes, E. P., V. A. Luckow, and L. Hanley-Bowdoin.** 1992. A geminivirus replication protein is a sequence-specific DNA binding protein. Plant Cell **4:**597–608.
13. **Frey, P. M., N. G. Scharer-Hernandez, J. Fütterer, I. Potrykus, and J. Puonti-Kaerlas.** 2001. Simultaneous analysis of the bidirectional African cassava mosaic virus promoter activity using two different luciferase genes. Virus Genes **22:**231–242.
14. **Frischmuth, S., T. Frischmuth, and H. Jeske.** 1991. Transcript mapping of Abutilon mosaic virus, a geminivirus. Virology **185:**596–604.
15. **Fütterer, J., K. Gordon, P. Pfeiffer, H. Sanfaçon, B. Pisan, J.-M. Bonneville, and T. Hohn.** 1989. Differential inhibition of downstream gene expression by the cauliflower mosaic virus 35S RNA leader. Virus Genes **3:**45–55.
16. **Gröning, B. R., R. J. Hayes, and K. W. Buck.** 1994. Simultaneous regulation of tomato golden mosaic virus coat protein and AL1 gene expression: expression of the AL4 gene may contribute to suppression of the AL1 gene. J. Gen. Virol. **75:**721–726.

17. **Haley, A., X. Zhan, K. Richardson, K. Head, and B. Morris.** 1992. Regulation of the activities of African cassava mosaic virus promoters by the AC1, AC2, and AC3 gene products. Virology **188:**905–909.
18. **Hanley-Bowdoin, L., J. S. Elmer, and S. G. Rogers.** 1988. Transient expression of heterologous RNAs using tomato golden mosaic virus. Nucleic Acids Res. **16:**10511–10528.
19. **Hanley-Bowdoin, L., J. S. Elmer, and S. G. Rogers.** 1989. Functional expression of the leftward open reading frames of the A component of tomato golden mosaic virus in transgenic tobacco plants. Plant Cell **1:**1057–1067.
20. **Hanley-Bowdoin, L., S. B. Settlage, B. M. Orozco, S. Nagar, and D. Robertson.** 1999. Geminiviruses: models for plant DNA replication, transcription, and cell cycle regulation. Crit. Rev. Plant Sci. **18:**71–106.
21. **Higo, K., Y. Ugawa, M. Iwamoto, and T. Korenaga.** 1999. Plant *cis*-acting regulatory DNA elements (PLACE) database: 1999. Nucleic Acids Res. **27:** 297–300.
22. **Hofer, J. M., E. L. Dekker, H. V. Reynolds, C. J. Woolston, B. S. Cox, and P. M. Mullineaux.** 1992. Coordinate regulation of replication and virion sense gene expression in wheat dwarf virus. Plant Cell **4:**213–223.
23. **Hong, Y., K. Saunders, M. R. Hartley, and J. Stanley.** 1996. Resistance to geminivirus infection by virus-induced expression of dianthin in transgenic plants. Virology **220:**119–127.
24. **Hong, Y., and J. Stanley.** 1995. Regulation of African cassava mosaic virus complementary-sense gene expression by N-terminal sequences of the replication-associated protein AC1. J. Gen. Virol. **76:**2415–2422.
25. **Hung, H. C., and I. T. Petty.** 2001. Functional equivalence of late gene promoters in bean golden mosaic virus with those in tomato golden mosaic virus. J. Gen. Virol. **82:**667–672.
26. **Jacob, S. S., R. Vanitharani, A. S. Karthikeyan, Y. Chinchore, P. Thillaichidambaram, and K. Veluthambi.** 2003. *Mungbean yellow mosaic virus*-Vi agroinfection by codelivery of DNA A and DNA B from one *Agrobacterium* strain. Plant Dis. **83:**247–251.
27. **Karthikeyan, A. S., R. Vanitharani, V. Balaji, S. Anuradha, P. Thillaichidambaram, P. V. Shivaprasad, C. Parameswari, V. Balamani, M. Saminathan, and K. Veluthambi.** 2004. Analysis of an isolate of Mungbean yellow mosaic virus (MYMV) with a highly variable DNA B component. Arch. Virol. **149:**1643–1652.
28. **Kozak, M.** 1991. A short leader sequence impairs the fidelity of initiation by eukaryotic ribosomes. Gene Expr. **1:**111–115.
29. **Kozak, M.** 2002. Pushing the limits of the scanning mechanism for initiation of translation. Gene **299:**1–34.
30. **Lorković, Z. J., D. A. Wieczorek Kirk, M. H. Lambermon, and W. Filipowicz.** 2000. Pre-mRNA splicing in higher plants. Trends Plant Sci. **5:**160–167.
31. **Lucioli, A., E. Noris, A. Brunetti, R. Tavazza, V. Ruzza, A. G. Castillo, E. R. Bejarano, G. P. Accotto, and M. Tavazza.** 2003. Tomato yellow leaf curl Sardinia virus rep-derived resistance to homologous and heterologous geminiviruses occurs by different mechanisms and is overcome if virus-mediated transgene silencing is activated. J. Virol. **77:**6785–6798.
32. **Morinaga, T., M. Ikegami, and K. Miura.** 1993. The nucleotide sequence and genome structure of mung bean yellow mosaic geminivirus. Microbiol. Immunol. **37:**471–476.
33. **Morris, D. R., and A. P. Geballe.** 2000. Upstream open reading frames as regulators of mRNA translation. Mol. Cell. Biol. **20:**8635–8642.
34. **Mullineaux, P. M., J. E. Rigden, I. B. Dry, L. R. Krake, and M. A. Rezaian.** 1993. Mapping of the polycistronic RNAs of tomato leaf curl geminivirus. Virology **193:**414–423.
35. **Pawlowski, K., R. Kunze, S. DeVries, and T. Bisseling.** 1994. Isolation of total, poly(A) and polysomal RNA from plant tissues, p. D5/1–D5/13. *In* S. B. Gelvin and R. A. Schilperoort (ed.), Plant molecular biology manual. Kluwer Academic Publishers, Dordrecht, The Netherlands.
36. **Petty, I. T. D., R. H. A. Coutts, and K. W. Buck.** 1988. Transcriptional mapping of the coat protein gene of tomato golden mosaic virus. J. Gen. Virol. **69:**1359–1365.
37. **Pilartz, M., and H. Jeske.** 2003. Mapping of Abutilon mosaic geminivirus minichromosomes. J. Virol. **77:**10808–10818.
38. **Pooggin, M. M., T. Hohn, and J. Fütterer.** 2000. Role of a short open reading frame in ribosome shunt on the cauliflower mosaic virus RNA leader. J. Biol. Chem. **275:**17288–17296.
39. **Rothnie, H. M.** 1996. Plant mRNA 3′-end formation. Plant Mol. Biol. **32:** 43–61.
40. **Ruiz-Medrano, R., R. G. Guevara-Gonzalez, G. R. Argüello-Astorga, Z. Monsalve-Fonnegra, L. R. Herrera-Estrella, and R. F. Rivera-Bustamante.** 1999. Identification of a sequence element involved in AC2-mediated transactivation of the pepper huasteco virus coat protein gene. Virology **253:** 162–169.
41. **Ryabova, L. A., M. M. Pooggin, and T. Hohn.** 2002. Viral strategies of translation initiation: ribosomal shunt and reinitiation. Prog. Nucleic Acid Res. Mol. Biol. **72:**1–39.
42. **Rybicki, E. P., R. W. Briddon, J. K. Brown, C. M. Fauquet, D. P. Maxwell, B. D. Harrison, P. G. Markham, D. M. Bisaro, D. Robinson, and J. Stanley.** 2000. Family *Geminiviridae*, p. 285–297. *In* M. H. V. van Regenmortel, C. M. Fauquet, D. H. L. Bishop, et al. (ed.), Virus taxonomy: classification and nomenclature of viruses. Academic Press, New York, N.Y.
43. **Schalk, H. J., V. Matzeit, B. Schiller, J. Schell, and B. Gronenborn.** 1989. Wheat dwarf virus, a geminivirus of graminaceous plants needs splicing for replication. EMBO J. **8:**359–364.
44. **Simpson, G. G., and W. Filipowicz.** 1996. Splicing of precursors to mRNA in higher plants: mechanism, regulation and sub-nuclear organisation of the spliceosomal machinery. Plant Mol. Biol. **32:**1–41.
45. **Sunter, G., and D. M. Bisaro.** 1989. Transcription map of the B genome component of tomato golden mosaic virus and comparison with A component transcripts. Virology **173:**647–655.
46. **Sunter, G., and D. M. Bisaro.** 1991. Transactivation in a geminivirus: AL2 gene product is needed for coat protein expression. Virology **180:**416–419.
47. **Sunter, G., and D. M. Bisaro.** 1992. Transactivation of geminivirus AR1 and BR1 gene expression by the viral AL2 gene product occurs at the level of transcription. Plant Cell **4:**1321–1331.
48. **Sunter, G., and D. M. Bisaro.** 1997. Regulation of a geminivirus coat protein promoter by AL2 protein (TrAP): evidence for activation and derepression mechanisms. Virology **232:**269–280.
49. **Sunter, G., and D. M. Bisaro.** 2003. Identification of a minimal sequence required for activation of the tomato golden mosaic virus coat protein promoter in protoplasts. Virology **305:**452–462.
50. **Sunter, G., W. E. Gardiner, and D. M. Bisaro.** 1989. Identification of tomato golden mosaic virus-specific RNAs in infected plants. Virology **170:**243–250.
51. **Sunter, G., M. D. Hartitz, and D. M. Bisaro.** 1993. Tomato golden mosaic virus leftward gene expression: autoregulation of geminivirus replication protein. Virology **195:**275–280.
52. **Sunter, G., M. D. Hartitz, S. G. Hormuzdi, C. L. Brough, and D. M. Bisaro.** 1990. Genetic analysis of tomato golden mosaic virus: ORF AL2 is required for coat protein accumulation while ORF AL3 is necessary for efficient DNA replication. Virology **179:**69–77.
53. **Sunter, G., D. C. Stenger, and D. M. Bisaro.** 1994. Heterologous complementation by geminivirus AL2 and AL3 genes. Virology **203:**203–210.
54. **Townsend, R., J. Stanley, S. J. Curson, and M. N. Short.** 1985. Major polyadenylated transcripts of cassava latent virus and location of the gene encoding coat protein. EMBO J. **4:**33–37.
55. **Trinks, D., R. Rajeswaran, P. V. Shivaprasad, R. Akbergenov, E. Oakley, K. Veluthambi, T. Hohn, and M. M. Pooggin.** 2005. Suppression of silencing by a geminivirus nuclear protein, AC2, correlates with transactivation of host genes. J. Virol. **79:**2517–2527.
56. **Vanitharani, R., P. Chellappan, J. S. Pita, and C. M. Fauquet.** 2004. Differential roles of AC2 and AC4 of cassava geminiviruses in mediating synergism and suppression of posttranscriptional gene silencing. J. Virol. **78:** 9487–9498.
57. **Vanitha Rani, R., A. S. Karthikeyan, S. Anuradha, and K. Veluthambi.** 1996. Genome homologies among geminiviruses infecting Vigna, cassava, Acalypha, Croton and Vernonia. Curr. Sci. (India) **70:**63–69.
58. **Voinnet, O., Y. M. Pinto, and D. C. Baulcombe.** 1999. Suppression of gene silencing: a general strategy used by diverse DNA and RNA viruses of plants. Proc. Natl. Acad. Sci. USA **96:**14147–14152.
59. **Xie, M., Y. He, and S. Gan.** 2001. Bidirectionalization of polar promoters in plants. Nat. Biotechnol. **19:**677–679.
60. **Zhan, X. C., A. Haley, K. Richardson, and B. Morris.** 1991. Analysis of the potential promoter sequences of African cassava mosaic virus by transient expression of the beta-glucuronidase gene. J. Gen. Virol. **72:**2849–2852.